Steel and Composite Structures, Vol. 6, No. 6 (2006) 493-512
DOI: http://dx.doi.org/10.12989/scs.2006.6.6.493

Seismic behaviour of steel beam-to-column joints with column web stiffening

A. L. Ciutina† and D. Dubina‡

The "Politehnica" University of Timisoara, Romania

(Received July 21, 2005, Accepted July 3, 2006)

Abstract. The present paper summarizes the experimental research carried out at the "Politehnica" University of Timisoara, Romania, with the scope of investigating the influence of different column web stiffening solutions on the performance of beam-to-column joints of Moment Resisting Steel Frames. The response parameters, such as resistance, rigidity and ductility were examined. Five different types of panel web stiffening were compared with regard to a reference test. A quasi-linear relationship between the moment capacity and the total shear area of the web panel was observed from the experimental tests while the initial rigidity increased non-proportionally with the same area. Comparisons are presented of the experimental tests with the mathematical model developed by Krawinkler and with the model stipulated in Eurocode 3 Part 1.8. These comparisons showed a generally good agreement in the case of moment capacity, while the computed rigidities were always greater than the experimental rigidities.

Keywords: column web panel; supplementary plate; rigidity; shear resistance; moment capacity; seismic codes.

1. Introduction

Lateral loads, e.g., wind and earthquake loads, acting on Moment Resisting Steel Frames (MRSF) introduce high shear forces into the Column Web Panels (CWP) of joints. Thus, rather than forming plastic flexural hinges in beams or columns, the dissipation of input energy is located into the CWP. In the case of internal joints, due to opposite moments acting at the ends of the connected beams, the shear effect is more pronounced than that of external joints. Depending on the connection typology, the CWP can supply the most important part or even the entire rotation capacity of the joint (Dubina 2001). The resulting web deformations have an important effect on the overall structural response, leading sometimes to important second-order structural effects. As shown by Schneider and Amidi (1998), in the case of a regular MRSF, column web panel distortions can influence the total lateral drift by about 10% and the base shear strength by about 30%.

Various experimental tests on beam-to-column joints have revealed important features regarding CWP behaviour, particularly the following (El Tawil *et al*. 1998):

(1) A sheared CWP develops a maximum strength significantly greater than the yielding strength, due to its strain-hardening effect.

†Senior Lecturer, E-mail: ciuti@constructii.west.ro
‡Professor, Corresponding author, E-mail: dubina@constructii.west.ro

(2) In the inelastic range, CWPs show a very ductile behaviour, both for monotonic and cyclic loading. In the case of cyclic loading, the hysteretic loops remain stable even for large deformations.

(3) However, large inter-story drifts are required for attaining the full-resistance of a CWP. For this reason, the maximum shear capacity of a CWP is not easily attained.

Krawinkler *et al.* (1971) proposed an analytical mathematical model on the equivalent non-linear springs for I and H steel profiles in order to simulate the CWP behaviour for structural analysis. This represents a three-linear model and has been derived for modelling CWP behaviour in terms of shear force (V) and panel distortion (γ). The adapted model was adopted for several American seismic norms, including the recent version of AISC (2005) section 9.3.

In the latest version of Eurocode 8 Part 1 (2003) the possibility of dissipating the energy under hysteretic form is cited as conceivable within the beam-to-column joint (see clauses 6.5.2(3) and (5)) so even in a web panel of a column. However, the Eurocode takes a prudent position regarding a situation of this kind, not authorising angular distortions higher than 30% of the total plastic rotational capacity of the dissipative zone adjacent to the joint (see clause 6.6.4 (4)). Other studies (Lu *et al*. 2000) have estimated that a contribution of the CWP rotation of 50% from the total joint rotation is quite reasonable, especially in the case of a welded connection.

Concerning the shear resistance of a panel, Eurocode 8-1 (2003) is based directly on Eurocode 3, Part 1.8 (2003) (see clause 6.6.3(6) of Eurocode 8). Especially under seismic conditions, the beam-to-column joint resistance could depend on the resistance of the CWP. In order to increase the resistance of the CWP, supplementary column web plates could be used to increase both the strength and the stiffness of the joint. Doing so may also influence the ductility of the joint. In this scope, an adequate design is needed for finding the best resistance/ductility ratios.

By Eurocode 3, Part 1.8, when designing a reinforced CWP, the effective additional area is limited to a single supplementary plate having a thickness equal to that of the web column profile. However, other studies (Dubina *et al*. 2002) have shown that in the case of cruciform cross-sectional columns, the entire shear area (e.g. the web and the two adjacent column flanges) should be considered in shear.

Starting from the preceding considerations, twelve experimental tests were performed at the "Politehnica" University of Timisoara, in order to investigate the influence of column web stiffening on overall beam-to-column joint behaviour (welded internal joints). Five different types of web stiffening were compared to a reference (unstiffened) case, as will be described. For each case of stiffening, monotonic and cyclic loadings were applied. Finally, using an unstiffened CWP by transverse stiffeners but reinforced by supplementary plates, the validity of the resistance and stiffness formulae given in Eurocode 3 were examined, with respect to seismic applications, while preserving the conditions of Eurocode 8.

2. General characteristics of a CWP element

A column web panel can be considered as basically a rotational element that transfers moments between the column and the beams framed into a specific joint. The boundary forces (see Fig. 1) on a panel zone can be transformed into an approximate equivalent shear force, as follows:

$$V_{wp} = \frac{M_{b1} - M_{b2}}{z} - \frac{V_{c1} - V_{c2}}{2} \tag{1}$$

Where: M_{b1} and M_{b2} are the moments given by the beams, and V_{c1} and V_{c2} are the shear forces in the column;
z is the level arm of the panel (here being the distance between the mid-thickness of beam flanges).

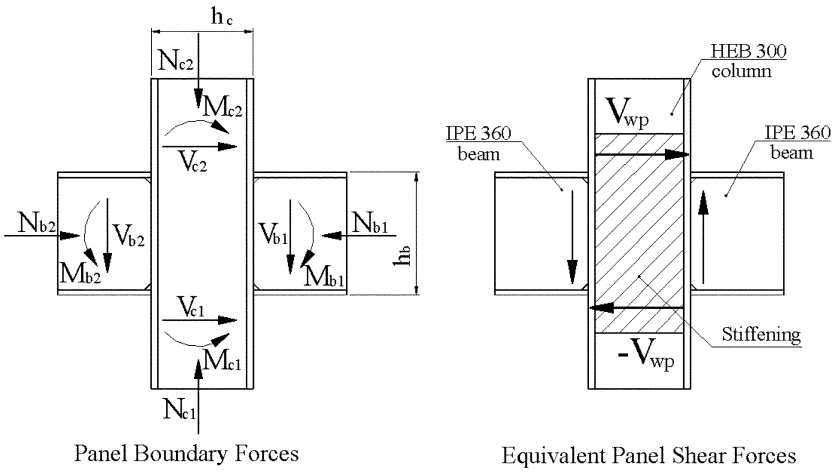

Fig. 1 Boundary forces and shear forces of a CWP

The design resistance of a panel joint is expressed in terms of rotational rigidity and yield shear strength. The hysteretic rules and the rotation capacity are the main supplementary parameters that characterize the cyclic behaviour. By Eq. (1), the panel zone force V_{wp} versus the panel zone deformation can be transferred into the panel zone moment M_{cwp} versus the panel zone distortion, γ.

$$M_{cwp} = V_{wp}z \tag{2}$$

This definition is also used for computing the CWP moment for the experimental tests and for characterizing the specimens' behaviour together with the angular distortion defined in the following sections.

3. Specimens, testing set-up and loading protocol

The aim of the experimental test was to observe the influence of different types of stiffening versus the global behaviour of CWPs. For this purpose, five typologies of stiffening were tested, as follows:

- One-sided supplementary plate specimens (CP-IP series), which represent the typical European CWP stiffening method. The width of the supplementary plate was limited to 150 mm, consistent with the ENV version of Eurocode 3 1992 (see paragraph J.2.2), while the supplementary plate thickness was 10 mm and fillet welded over the entire perimeter.
- Two-sided plate specimens (CP-IIP series), which were composed of two identical supplementary plates welded (by fillet weld) symmetrical to the column web.
- Two larger plate specimens (CP-IIPL series) which were also comprised two identical plates, but were larger than those of the CP-IIP series in order to cover the entire column web, up to the root fillet of the column profile. The width of the plates was 220 mm, and the weld was extended to reach the root fillet.
- Two distanced plate specimens (CP-IIPD series). In this series, the two supplementary plates were distanced from the column web and welded by fillet welds to the column flanges, resulting in a width of 260 mm. This practice is largely used in the United States and has lately been adopted in

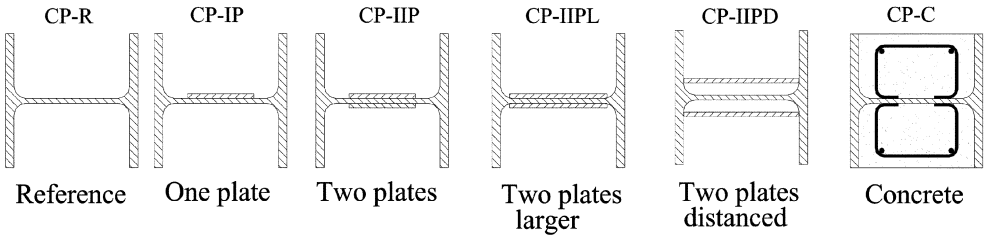

Fig. 2 Typologies of a CWP specimen series – cross section through the columns

European design guides.

- In-filled Concrete specimens (CP-C series), in which the web panels were stiffened by reinforced concrete. The steel stirrups (Φ = 6 mm) were welded onto column web and attached to longitudinal reinforcements: 2Φ 12 mm re-bars (see Fig. 2).

All the stiffened specimens were compared to a reference specimen with no CWP stiffening, namely, the series CP-R. Table 1 provides a description of the experimental tests. For all the specimens, hot-rolled sections of IPE 360 (S 355) and HEB 300 (S235) were used for the beams and the columns, respectively. Fig. 2 shows the typology of the tested specimens. Specimens were designed in such a way that the CWP was always the weakest component for the specific action. The thickness of all the supplementary plates was 10 mm. As already mentioned, no transverse stiffeners were used on the specimens.

The beam-to-column connections were made in shop using full-penetration double bevel butt welds, with quality control. A detail of the edge preparation is given in Fig. 3. For the supplementary plates, fillet welds were used.

The test setup is shown in Fig. 4. Statically, the joint is simply supported at the two ends of the connected beams and pinned at the column base. Thus, equal and opposite moments form in the beams, causing shearing of the CWP.

For this type of tests the representative curve is expressed in terms of "moment M_{cw} – panel distortion γ". The corresponding panel moment - M_{cw} was computed both from the geometry of the testing equipment

Table 1 Description of the CWP tests

Test reference	Reinforcing type	Number of supplementary plates	Width of the supplementary plates	Loading
CP-R-M	None	---	---	Monotone
CP-R-C	None	---	---	Cyclic - ECCS
CP-C-M	Concrete	---	---	Monotone
CP-C-C	Concrete	---	---	Cyclic - ECCS
CP-IP-M	Supplementary plate	1	150 mm	Monotone
CP-IP-C	Supplementary plate	1	150 mm	Cyclic - ECCS
CP-IIP-M	Supplementary plate	2	150 mm	Monotone
CP-IIP-C	Supplementary plate	2	150 mm	Cyclic - ECCS
CP-IIPL-M	Supplementary plate	2	220 mm	Monotone
CP-IIPL-C	Supplementary plate	2	220 mm	Cyclic - ECCS
CP-IIPD-M	Supplementary plate	2	260 mm	Monotone
CP-IIPD-C	Supplementary plate	2	260 mm	Cyclic - ECCS

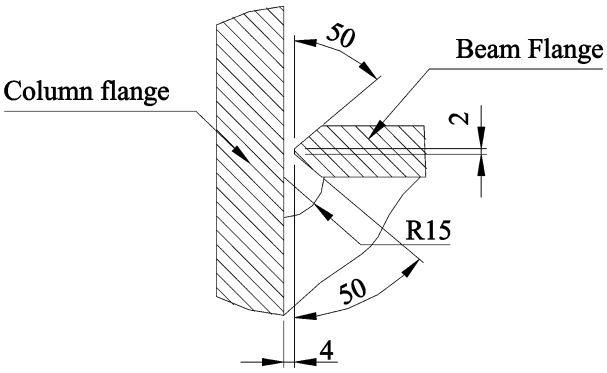

Fig. 3 Detail of edge preparation for beam flange-to-column weld

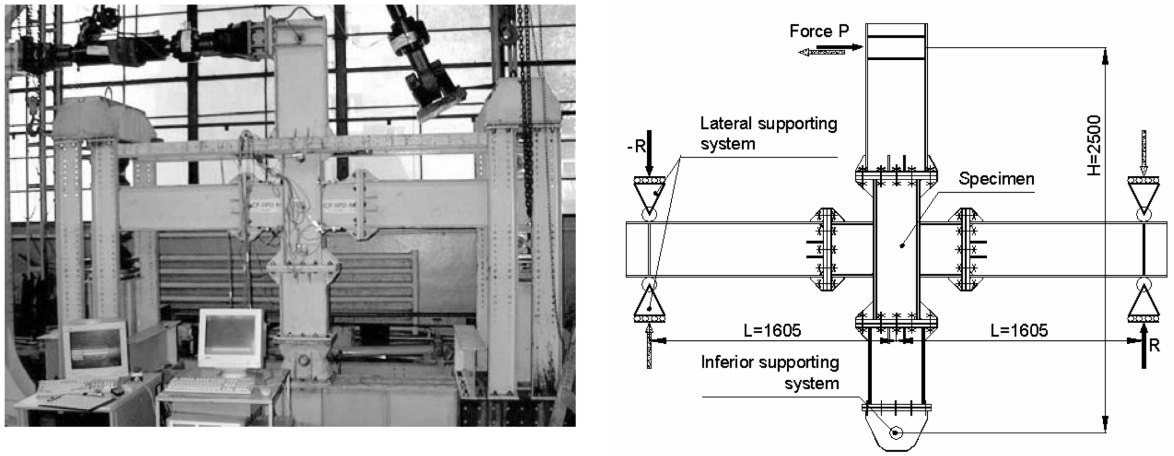

Fig. 4 Test set up

and from the applied force by the actuator (by Eqs. (1) and (2)) at the outer face of the column. The panel distortion - γ was calculated starting from the diagonal LVDT transducers placed on the diagonals of the web panel.

For each series of specimens the ECCS Recommendations Complete Procedure (1986) (see Fig. 5) was applied, beginning with a monotonic test. Then, based on the conventional yielding characteristics computed based on the monotonic test, a cyclic procedure was applied on a second specimen. The tests were conducted under displacement control. Specimen failure was considered to have occurred when the maximum force reached during a cycle was smaller than 50% of the maximum load attained.

In order to establish the actual mechanical characteristics of the CWP elements prior to testing, samples of material, concrete and steel (column web and flanges and supplementary plates), were tested. Table 2 provides the characteristic values of the tensile tests. For the design of the joints, S235 steel was chosen. For the concrete, a nominal compressive strength of 31.72 N/mm² was obtained for a design C25/30 concrete.

Although, in reality, there is axial force in the column, its influence on the sheared CWP is small even at important values of the axial forces. According to Krawinkler (1971), the coefficient that affects the shear resistance of a CWP due to the axial force is given by $\sqrt{1-(N_{Ed}/N_{pl,R})^2}$, as will be explained

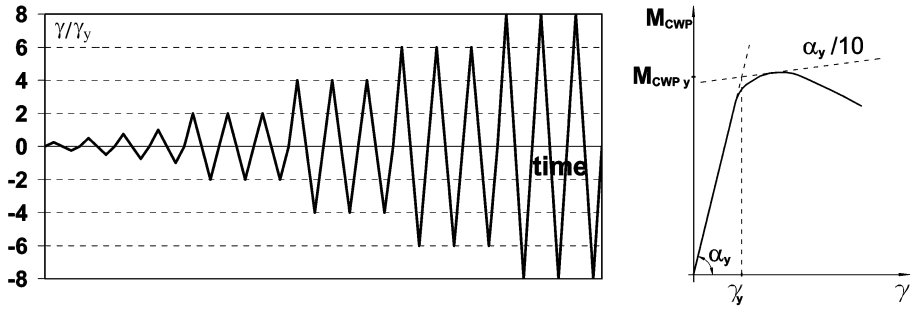

Fig. 5 ECCS loading procedure and determination of yielding characteristics

Table 2 Mechanical characteristics of steel elements

Element		f_y [N/mm²]	f_u [N/mm²]	A [%]
Column	Web	301.8	451.8	35.5
	Flange	260.5	425.3	30.9
Supplementary plate		276.1	407.1	29.3
Stirrups Φ 6 mm		268.3	538.8	27.3

later. This coefficient remains over 0.9, even when the axial force in the column is 0.4 $N_{pl,R}$. In consequence, it was decided that for the tests reported here no axial force was introduced into the column.

4. Data processing

Fig. 6 shows the instrumentation used to determine the characteristic curve "moment-distortion" of the panel, in order to distinguish the different possible contributions. For this purpose, the transducers 3 to 6 were used to establish the relative displacements immediately adjacent to the panel.

Transducers 1 and 2 (see Dubina *et al.* 2001), which were diagonally fixed on the panel, provided the panel zone rotation γ at the level of beam flanges as:

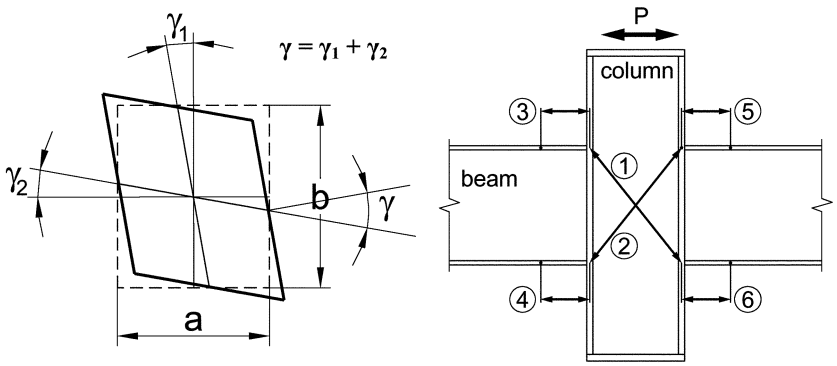

Fig. 6 Definition of panel zone rotation: Basic instrumentation for determining the distortion of a panel zone

$$\gamma = \frac{\sqrt{a^2 + b^2} \cdot (\Delta_1 + \Delta_2)}{2 \cdot a \cdot b} \tag{3}$$

In Eq. (3), a and b are the horizontal and vertical dimensions between the measuring points, whereas Δ_1 and Δ_2 are the relative displacements (in absolute value) recorded by the transducers 1 and 2 respectively. Note that, in the absence of transverse stiffeners, the value of γ integrates the complementary deformations due to local tension and compression in the column web at the level of beam flanges.

The bending moment for each part of the beam, defined at the beam-to-column connection was computed starting from the support reactions $\pm R$ and deduced from the force P exerted by the actuator:

$$M_{b1} = -M_{b2} = R\left(L - \frac{h}{2}\right) = -\frac{PH}{2L}\left(L - \frac{h}{2}\right) \tag{4}$$

In Eq. (4), H is the distance between the load application point and the bottom hinge, L is the distance between the column axis and each lateral beam hinge, and h is the height of the column section.

5. Test results

Table 3 presents the main results of the experimental tests. The following notations have been used:
$S_{j,ini}$: initial stiffness of the monotonic $M_{cw}(\gamma)$ curves or of envelope curves for the cyclic specimens;
$M_{cw,y}$: the yielding moment, as computed based on the ECCS procedure;
$M_{cw,max}$: the maximum resistance moment recorded during a test ;
γ_u: the maximum panel distortion, as computed for a drop of 20% in the maximum moment $M_{cw,max}$ (after attaining this value);
$S_{j,sh}$: the strain-hardening tangent stiffness (at an approximate distortion of 40 mrad), computed on the envelope curves for the cyclic tests;

Table 3 Principal results of the CWP tests

Specimen	$M_{cw,y}$ [kNm]		$M_{cw,max}$ [kNm]		$S_{j,ini}$ [kNm/rad]		γ_u [mrad]		$S_{j,sh}$ [kNm/rad]		W_p	No.
	Pos.	Neg.	Pos.	Neg.	Pos.	Neg.	Pos.	Neg.	Pos.	Neg.	[kNm rad]	cycles
CP-R-M		199.7		371.1		53163		142.4*		1950	---	---
CP-R-C	220.9	216.5	346.9	368.4	53985	54060	79.7	84	2371	2190	1521	42
CP-C-M		251.2		414.6		84695		167.2*		1258	---	---
CP-C-C	270.1	273.4	371.5	389.3	85703	87954	74.8	84	1370	1189	1660	44
CP-IP-M		278.1		472.5		55315		89.3*		2025	---	---
CP-IP-C	296.7	299.6	444.6	454.7	64988	72259	54.5	56	4053	4224	635	22
CP-IIP-M		351.6		536.6		56314		177.3		2480	---	---
CP-IIP-C	370.3	367.4	520.8	532.5	64805	69862	68	70	4652	4179	821	22
CP-IIPL-M		450.4		700.2		72779		136.5		3739	---	---
CP-IIPL-C	476.7	484.6	655.6	664.1	85872	75423	61	61	5369	5338	684	19
CP-IIPD-M		481.1		731.7		100215		84.3		4240	---	---
CP-IIPD-C	512.9	530.7	727.2	730.5	104020	105586	46.4	46.1	6848	6392	636	21

*Computed at the attainment of the actuator limit.

W_p: the total cumulated plastic energy in the cyclic loading;
No. cycles: the number of cycles performed until failure.

5.1. Results of the monotonic specimens

Fig. 7 shows the graphical representation of the corresponding $M_{cw}(\gamma)$ curves for monotonic specimens, completing in this way the data offered in Table 3.

As expected, the yielding and the maximum resistant moments increased from the reference specimen CP-R-M to the specimen having the maximum shear area, CP-IIPD-M presenting the maximum shear area. In contrast, this tendency was not so evident in the case of the initial rigidity, $S_{j,ini}$, which was almost the same for the R, IP, and IIP monotonic specimens, but significantly greater for specimens with larger and distanced supplementary plates. As for the in-filled concrete specimen, the initial rigidity of the panel was increased with regard to the reference specimen, but this increase had no significant influence on the resistant moment. However, Simoes *et al.* (1999) proved that the total encasement of a steel column in concrete enables important increases of both the initial rigidity and the moment resistance of CWP.

We can note that the strain-hardening rigidities were also higher for the specimens having the greater shear area. However, a very small strain-hardening slope was observed for the specimen with a concrete encased web panel.

Although very important distortions of the CWP (until 0.15 rad.) were observed, no failures occurred in the panels. For all practical purposes, the actuator stroke limitation (approximately 35 cm) marked the end of the monotonic experiments. An example of joint distortion is given in Fig. 8 for the CP-IP-M specimen. The only exception observed was for the CP-IIPL-M specimen, where the connection failed, but side-away of the CWP.

For all the cases, it could be concluded that the monotonic tests showed a very good and stable monotonic behaviour, even with panel rotations of more than 100 mrad.

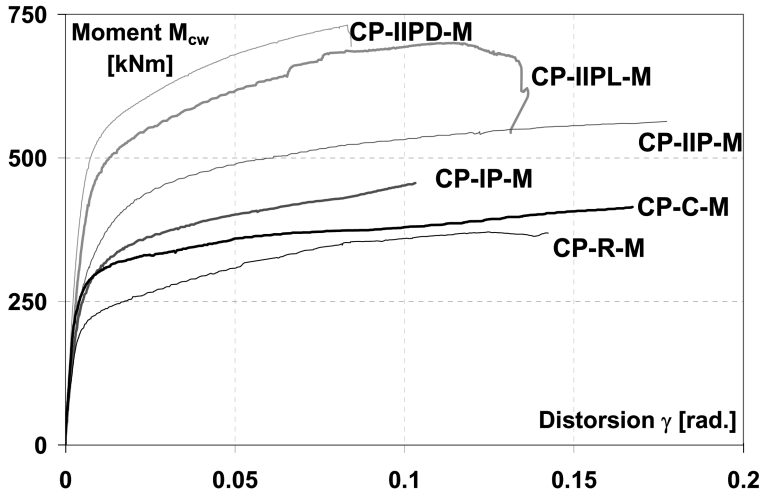

Fig. 7 Results of the monotonic tests

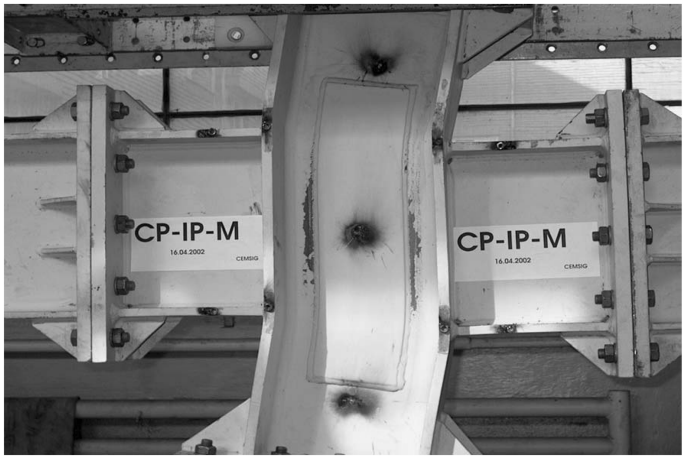

Fig. 8 Distortion of CP-IP-M specimen

5.2. Cyclic specimens

Table 3 also presents the numerical values of the main parameters for the cyclic tests, both for positive and negative branches. Fig. 9 shows the panel moment M_{cw} versus the panel distortion γ relationships, scaled at the same amplitudes. Fig. 9 also displays the failure modes for all cyclic specimens. As a general tendency, all the specimens showed very stable cyclic behaviours, with no degradation until failure. Generally, an ascending tendency similar to that of the monotonic tests of the maximum resistance was observed. However, a decrease of up to 10% of the maximum moments was observed for the cyclic specimens. On the other hand, the cyclic specimens were significantly stiffer during the elastic cycles. Therefore, major differences were recorded between the cases using the CP-IP-C specimen with a single supplementary plate and those using the CP-IIP-C specimen having supplementary plates on each side (positive and negative branches), as compared to the corresponding monotonic ones.

The CP-C-C specimen encased by concrete exhibits a particular behaviour for cyclic loading: although it showed almost the same elastic rigidity as the monotonic specimen and a "normal" degradation of the maximum moment, a visible cyclic degradation of the moment and plastic rigidity during the three cycles at equal amplitude was observed. This phenomenon was due to the degradation of the concrete in the first cycle with increased amplitude.

More clearly than the elastic rigidity, the hardening rigidity increased with the shear area during the cyclic tests, as presented in Table 3. Even where the values of hardening rigidities in the positive and negatives branches of the cyclic tests are different for the CWP specimens doubled by steel plates, they are generally greater than those obtained in the monotonic tests.

Mainly, two failure modes were observed for the cyclic specimens:

1. A ductile failure mode, observed for the case of reference CP-R-C and CP-C-C specimens. For these cases, small fissures began to form on the kinking zones situated on the external parts of the beam flange-to-column welds. As the distortion amplitude increased, the fissures advanced along the entire column flange thickness and then continued into the column web, forming lines parallel to the column flanges. Simultaneously, a horizontal fissure developed on a median line of the panel. The final crack pattern formed an "H" letter shape, as shown in Fig. 9. In addition to the

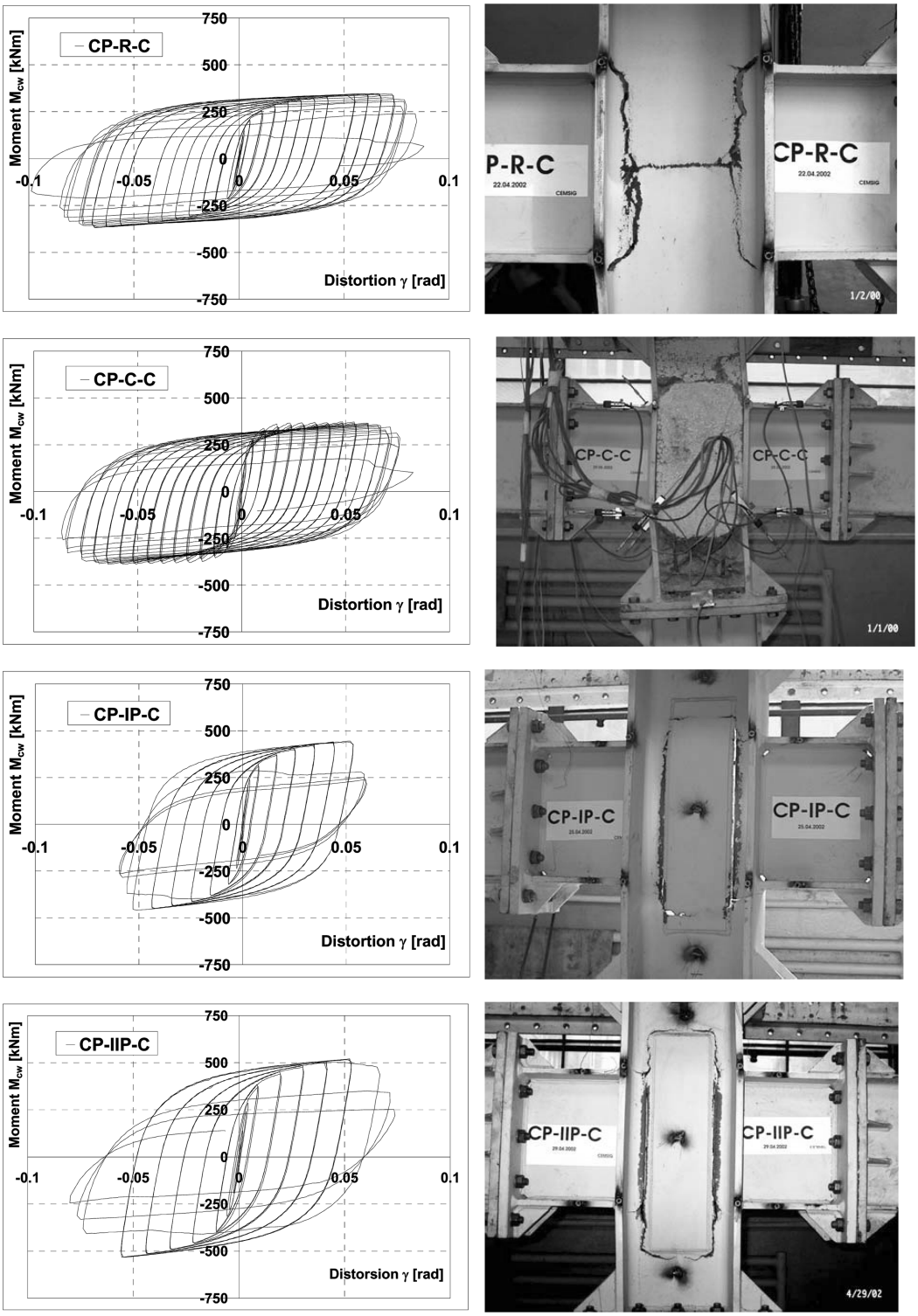

Fig. 9 Cyclic behaviour and failure mode of cyclic specimens

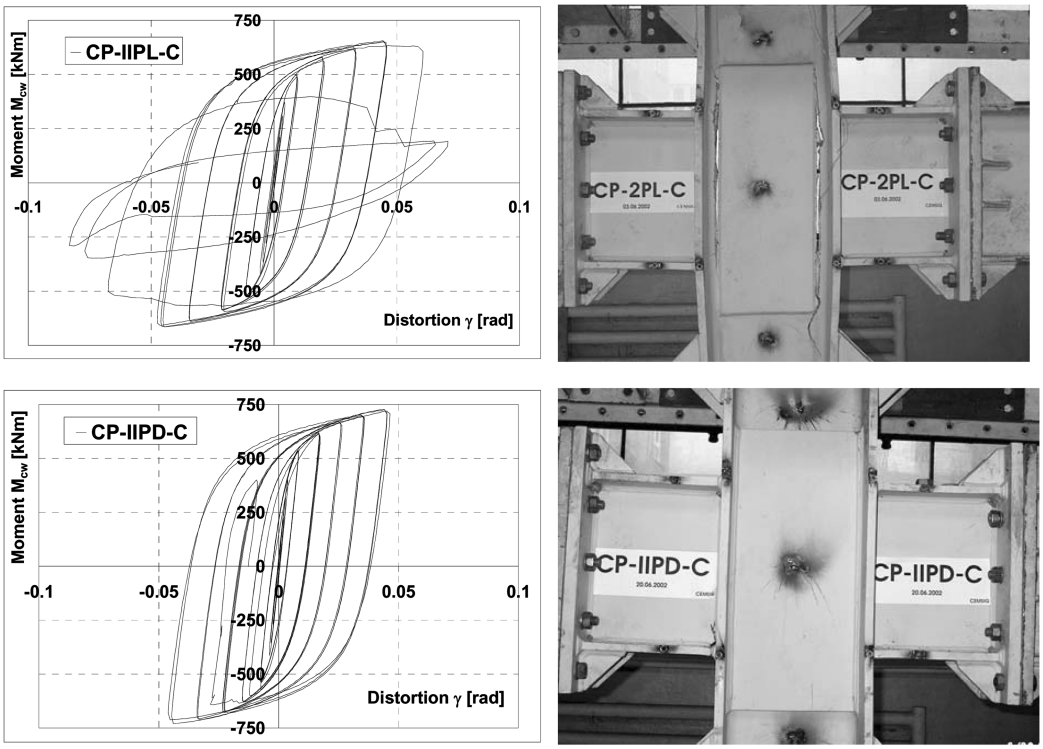

Fig. 9 (continued)

steel cracks, concrete fissures were observed in the concrete specimen from the beginning cycles. These fissures formed horizontally at the delimitation of the CWP. At higher values of distortion, failures of the stirrups in shear were observed.

2. Brittle failures, which were also observed during the other tests, except for the CP-IIPD-C specimen. For these specimens, initial fissures formed near the supplementary plates at the level of the column flanges. Vertical fissures rapidly propagated along the supplementary plates and produced a rapid degradation of the resistance.

In the case of the CP-IIPD-C specimen, failure occurred by a brittle rupture of a beam flange outside the CWP. This happened near the weld to the column flange, in the lateral part and within the heat affected zone of the beam flange weld. In subsequent cycles, the rupture tended to extend into the beam web.

The maximum panel distortions generally followed the joint failure mode. The greatest distortion values (84 mrad) were obtained for the CP-R and CP-C specimens. However, all the specimens exhibited a rotation greater than 35 mrad, a value considered as guaranteeing a "high ductility" behaviour of MRSF by Eurocode 8 (see clause 6.6.4(3)). In addition, even with the most stiffened specimen, the panel zone deformed properly in shear in order to dissipate the energy necessary to attain behaviour factors on the order of 6 (see clause 6.3.2 (1) of Eurocode 8).

The value of the cumulated energy (last column of Table 3) depends evidently on several parameters, e.g., the number of cycles performed and the cycle amplitudes. The maximum dissipated energy was obtained for the concrete in-filled specimen, followed by the reference specimen, in relation to their ductile behaviours and specific failure modes. In comparison, all the other specimens

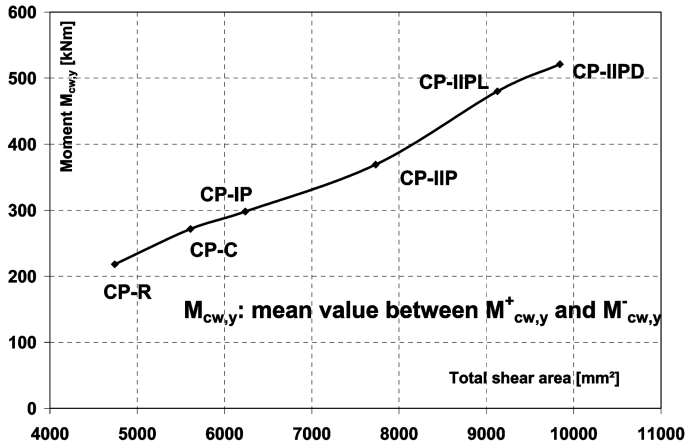

Fig. 10 Variation of conventional elastic moment (ECCS definition) with the total shear area

experienced an energy dissipation of about half. Although they had a greater resistance, their failure mode was brittle.

Briefly, the cyclically tested specimens exhibited very stable behaviour in all cases, and their respective resistances increased proportionally to the shear area. These specimens also had good ductility and strain-hardening ratios. Though failure was brittle for the stiffened specimens, this kind of failure is typically produced for relatively high values of plastic distortion.

Fig. 10 shows very clearly that the variation of the elastic moment $M_{cw,y}$ (determined by the ECCS procedure) increases quasi-linearly with the total shearing area. Here, total shear area refers to the shear area of the column section A_{vc} (computed according to paragraph 6.2.6.1(2) of Eurocode 3), augmented by the total section of the supplementary plate(s). Accordingly, the limitation specified in Eurocode 3 clause 6.2.6.1(6) was ignored here. In the particular case of the CP-C specimen, the shear area was computed by integrating the supplementary area comprised of the reinforcing stirrups present in the CWP.

The variation of the ultimate angular distortion with the total shear area is given in Fig. 11. By the exception of CP-IO specimen, this deformation capacity decreases almost linearly as the shear area

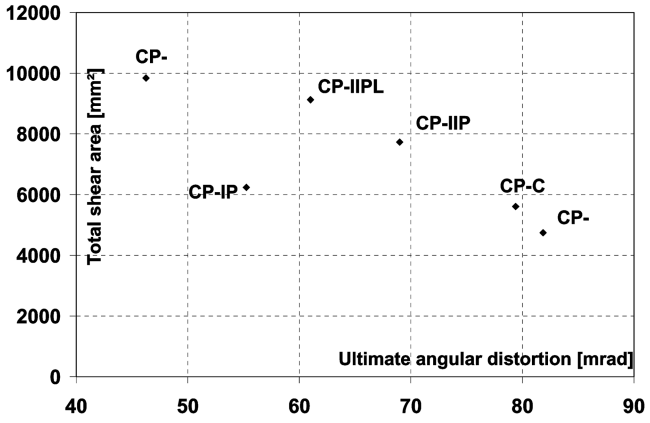

Fig. 11 Variation of the ultimate angular distortion with the total shear area

increases. It should be noted, however, that even in the worse case, the angular distortion stays above 40 mrad. The case of the CP-IP specimen (with a configuration that is evidently not recommendable) is explained by the weak resistance of the components under local tension and compression, i.e., the components situated between the supplementary plates and the fillet root of the steel profiles. Thus, a simple calculation according to Eurocode 3 Part 1.8, taking into account the interaction with the shearing (by factor ω from Table 6.3) confirms this explanation for the specimen CP-IP; it also shows that, for the case of the specimen CP-IIP, with two supplementary plates of limited width, it must in principle present the same weakness.

6. Comparison to theoretical models

In this section, the characteristics of the $M_{cw}(\gamma)$ curves of the monotonic specimens and of the envelopes of the cyclic curves are compared to the results given by two analytical approaches available for dimensioning the CWP in shear: Krawinkler's (1978) model and the design approach of Eurocode 3 Part 1.8.

Part 1-8 of Eurocode 3 allows the calculation of the initial stiffness $S_{j,ini}$ and of the resistant moment M_{wp}, for the column web in shear component of a connection as follows:

$$S_{j,int}^{(sh)} = 0,38EzA_{vc} \tag{5}$$

$$M_{cw,y} = \frac{0,9\, f_{y,wc} A_{vc}}{\sqrt{3}} z \tag{6}$$

In the foregoing equations, the following notations have been used:

A_{vc}: the column area subjected to shear, where the presence of supplementary plates allows the possibility of increasing its value, as follows: $A_{vc,\,\mathrm{sup}} = t_{wc} b_s$;

$f_{y,wc}$: the yielding strength of CW steel;

z: the level arm of the panel zone;

E: the elastic modulus of steel;

and the (sh) indices indicate the shearing effect.

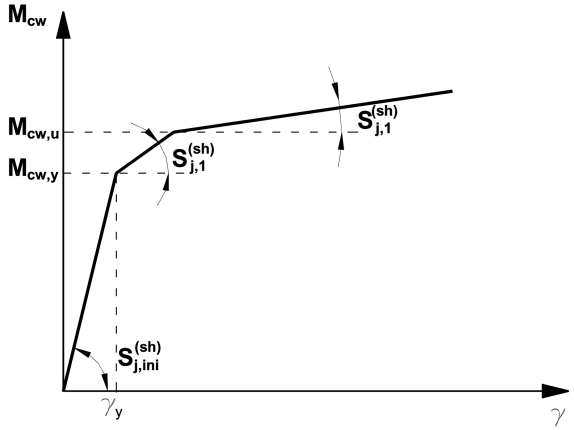

Fig. 12 Krawinkler's three-linear model

On the other hand, Krawinkler's model allows a three-linear modelling of the whole column web panel (see Fig. 12), as defined by the following characteristics:

- the elastic moment: $$M_{cw,y} = \frac{f_{y,wc} A_{vc}^*}{\sqrt{3}} z^* \quad (7)$$

- the maximum resistant moment: $$M_{cw,u} = M_{cw,y} + \frac{3,12\, f_{y,wc} b_{fc} t_{cf}^2}{\sqrt{3}} \quad (8)$$

- the tangent elastic stiffness: $$S_{j,ini}^{(sh)} = G A_{vc}^* z^* \quad (9)$$

- the tangent post-elastic stiffness: $$S_{j,1} = 1.04 G b_{cf} t_{cf}^2 \quad (10)$$

- the tangent strain-hardening stiffness: $$S_{j,2} = G_{st} A_{vc}^* z^* \quad (11)$$

In Eqs. (7)-(11), the following notations have been used:

b_{fc}, t_{fc}: the width and the thickness of the column's flange, respectively;

G, G_{st}: the shear modulus in shear of the column web respectively in elastic behaviour ($G = E/[2(1+\nu)]$) and in the strain-hardening phase - tangent modulus (with a G_{st} on the order of G/130), respectively;

A_{vc}^* and z^*: the shearing area and the level arm of the panel, respectively, defined by the author as:

$$A_{vc}^* = (h_c - t_{fc}) t_{wc} \quad (12)$$

$$z^* = h_b \quad (13)$$

h_b, h_c: the heights of the column and beam, respectively,

t_{wc} and t_{fc}: the thicknesses of the web and flanges, respectively.

Although the formulae for the two different approaches start from the same analytical models, some differences exist, i.e.:

- the effective shear area taken into consideration is different for the two approaches. While the Eurocode 3 approach considers the entire shear area of the hot-rolled profiles (including the root fillet and a part of the flanges for a width equal to $(t_{wc}+2r)t_{fc}$ (see 6.2.6(3) of EN 1993-1-1), the Krawinkler model uses a reduced value of $(h_c - t_{cf})t_{wc}$;
- the height of the level arm used is also different for the two approaches: Eurocode 3 uses a level arm height of $(h_b - t_{bf})$, while the level arm height used by Krawinkler is equal to the total beam height h_b.
- in Krawinkler's formulae, there is no explicit limitation concerning the supplementary plates on the column web;
- in Krawinkler's approach, the yielding moment takes into account the real axial load on the column (by the factor $\sqrt{1-(N_{Ed}/N_{pl,R})^2}$, where N_{Ed} is the normal axial load and $N_{pl,R}$ is the axial plastic resistance); in contrast, the Eurocode 8 stipulates that this effect could be negligible in the panel (by clause 6.6.3(6)).

It is important to note that, when taking into consideration the configuration of joints, specifically of those specimens without transverse stiffeners, the local effects of tension and compression must be

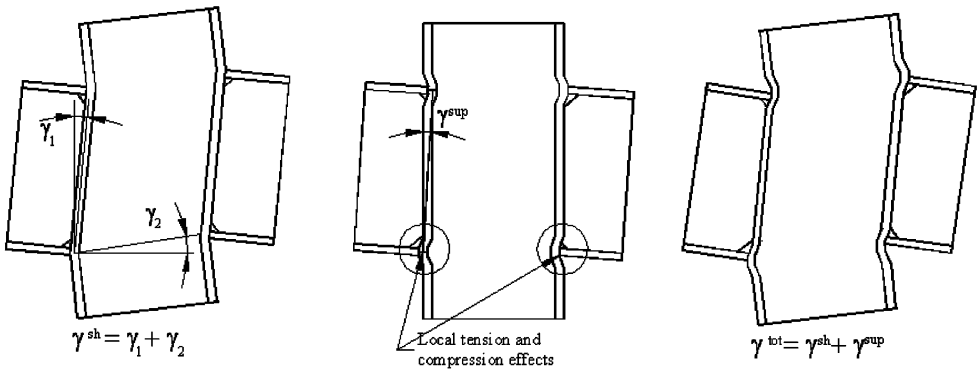

Fig. 13 Total distortion (including the local tension and compression effects)

included. These effects are illustrated in Fig. 13 as they correspond to the special conditions of the tests. This contribution can have a non-negligible influence on the global stiffness, even when supplementary plates are used to increase its resistance.

The effective stiffness of the CWP is evaluated by:

$$S_{j,ini} = \frac{1}{\dfrac{1}{S_{j,ini}^{(sh)}} + \dfrac{1}{2S_{j,e}^{(t,c)}}} \tag{14}$$

where $S_{j,e}^{(t,c)}$ is the stiffness due to the local effects of tension and compression at the level of the beam-to-column connection. This stiffness is given by:

$$S_{j,ini}^{(t,c)} = \frac{Ez^2}{\dfrac{1}{k_2} + \dfrac{1}{k_3}} \tag{15}$$

and where k_2 and k_3 are the values of the stiffness coefficients for compression and tension, respectively, as given in Eurocode 3 Part 1.8 (Table 6.11).

Table 4 presents the computed values of the yielding moments obtained by the two theoretical approaches compared to those deduced from the monotonic and cyclic tests (only steel specimens). It

Table 4 Comparison of the values of experimental results to theoretical approaches for elastic moments

Specimen Reference	Elastic moment M_y [kN m]					
	Tests $M_{cw,y}$		Eurocode 3: $M_{cw,y}$		Krawinkler	
	Mon.	Cycl.	with A_{conv}	with A_{tot}	$M_{cw,y}$	$M_{cw,u}$
CP-R	200.0	218.7	256.6	256.6	195.0	246.0
CP-IP	278.1	298.2	328.7	328.7	281.0	330.6
CP-IIP	351.6	368.8	340.8	407.6	366.9	415.8
CP-IIPL	450.4	480.6	376.7	473.9	447.1	495.6
CP-IIPD	481.1	521.8	397.9	508.7	493.0	541.3

Table 5 Comparison of the values of experimental results to theoretical approaches for initial stiffness

Specimen Reference	Initial Stiffness $S_{j,ini}$ [kN m/rad]					
	Tests		Eurocode 3		Krawinkler	
	Mon.	Cycl.	panel	panel + correction	panel	panel + correction
CP-R	53163	54023	130600	82618	85410	61900
CP-IP	55315	68624	170760	98690	126560	82330
CP-IIP	56314	67334	177340	101416	130850	84123
CP-IIPL	72779	80648	197380	138950	152050	114950
CP-IIPD	100215	104803	209210	144410	164160	121750

should be mentioned that, for the calculations obtained with Eurocode 3, two situations have been considered: the first uses conventional area A_{conv}, as stipulated by the norm and given by formula (5), while the second takes into consideration the entire shearing areas A_{tot}, which contain the shear area of the column profile and the entire area of the supplementary plates. A comparison of the experimental values $M_{cw,y}$ and the values computed using Eurocode 3 while considering the conventional shear area shows that the experimental values are clearly superior to the computed values for those cases where supplementary plate areas are important (namely, the cases involving the CP-IIPL and CP-IIPD specimens). Recall that Fig. 10 demonstrated the variation of the yielding moment with the shear area (quasi-linear variation). On the other hand, by considering the entire shear area, formula (6) of Eurocode 3 gives values higher than those resulting from the tests (and this is systematically for the case of monotonic tests). In comparison, the values of the yielding moment given by formula (7) of the Krawinkler approach (applied for the entire shearing area) seems to constitute a good compromise that always places the results in security with regard to the $M_{cw,y}$ values of the cyclic tests.

Theoretical and experimental stiffness values are compared in Table 5. For the theoretical models, a distinction must be made between the values $S_{j,ini}^{(sh)}$ of the panel and the corrected values according to Eq. (14). Taking into account the observations done before at the examination of Table 3, the supplementary area specified in Eurocode 3 Part 1.8 was adopted for the computation ($A_{vc,\sup} = t_{wc} b_s$ corresponding to a single supplementary plate, although two supplementary plates on each side of the web were used). By this hypothesis, formula (8) of the Krawinkler approach, corrected by taking into account the local tension and compression effects, leads to values that are closer to the experimental values than those obtained by the Eurocode. However, the general tendency of overestimating the experimental values persists, even under the improved conditions of this approach.

Up to now, Krawinkler's model has been used only for cases of elastic behaviour. It is instructive to make a more complete comparison of the tests on this model, which have the advantage of integrating the behaviour in the strain-hardening phase. This comparison is shown in Fig. 14, which also shows the results given by Eurocode 3 (with $S_{j,ini}$ computed by taking into account the correction signalled and with $M_{cw,y}$ computed by A_{tot}).

Generally, Krawinkler's model gives a good approximation of the experimental $M_{cw}(\gamma)$ curve for both cyclic and monotonic curves. The model also has the advantage of generating two values of the resistant moment to be used by engineers, according to their needs:

(1) when an over-resistant connection is chosen and, in consequence, an over-resistant CWP (with a dissipative zone located in the beam), it is wise to use the elastic moment $M_{cw,y}$ given by formula (7), which guarantees a limited distortion without risks of plastic deformations, and

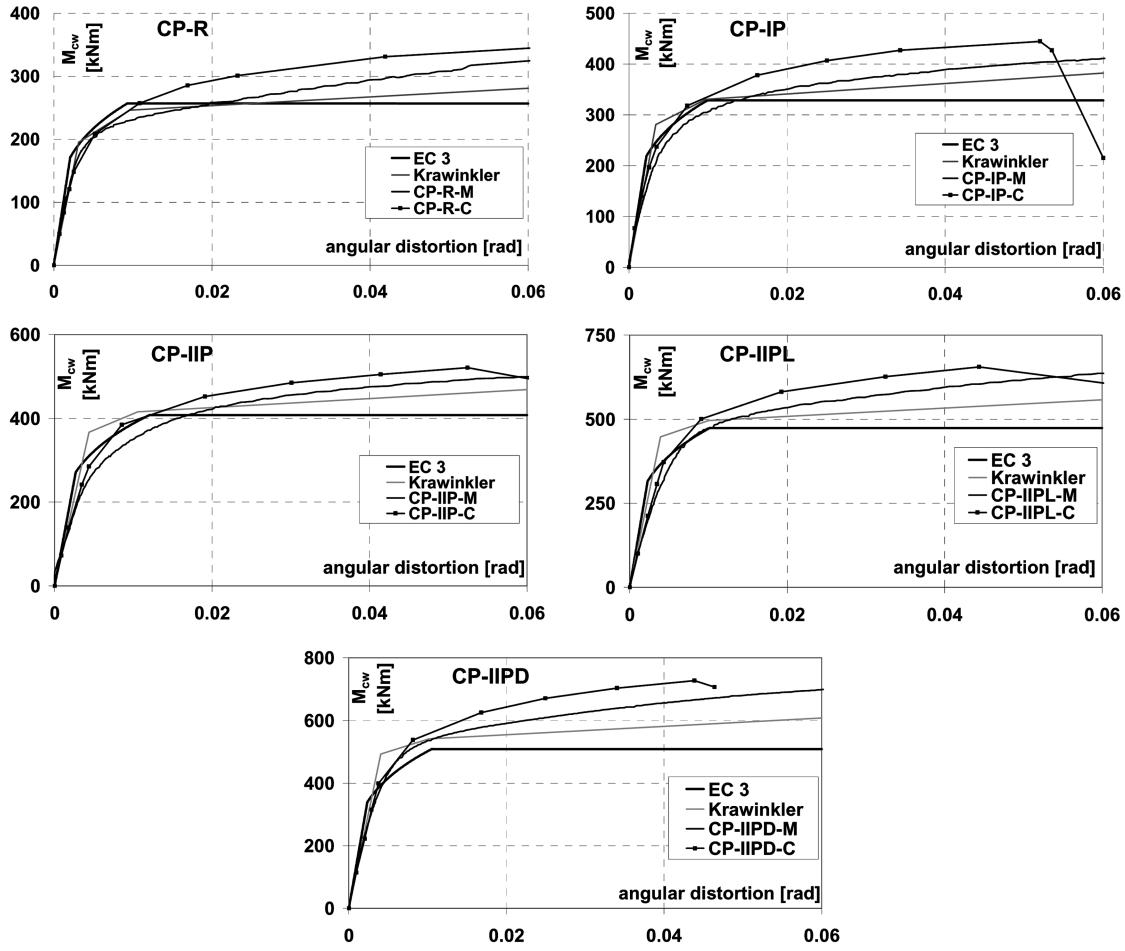

Fig. 14 Graphical comparisons of the monotonic and cyclic curves with those of the theoretical models

(2) when the CWP is part of a dissipative connection, and thus has partial-resistance in comparison to the beam, the plastic moment $M_{cw,u}$ from formula (8), and illustrated in Fig. 14, is judged reasonable to use (corresponding to a value of distortion of about 15-20 mrad), in the context of clause 6.6.4(4) of Eurocode 8-1, limiting the panel distortion to the global joint distortion.

7. Conclusions

This study has considered the influence of CWP reinforcing on the behaviour (in terms of resistance, stiffness, and ductility) of internal welded joints subjected to anti-symmetrical loading. Panels having no transversal stiffeners in the extension of the beam flanges were subjected to monotonic and cyclic loading (according to the ECCS procedure).

Different configurations of reinforcement with supplementary plates were considered. It was found that two supplementary plates distanced from the column web (fillet welded on the internal face of the column flanges, CP-IIPD series) provided the most efficient resistance, while conserving a deformation

capacity considered largely sufficient. The practice of encasing the web panel in concrete was ultimately shown to be relatively inefficient at increasing CWP resistance; however, a significant increase of the initial stiffness of the angular distortion was observed. Further studies of encased CWPs should be performed to confirm these results before any final conclusions can be drawn.

From a comparison of the experimental values obtained for different solutions of supplementary web plates tested and from the two analytical approaches, the following conclusions have been drawn:

(1) For the calculation of the initial stiffness of the panel, the limitation of the supplementary web plates stipulated in Eurocode 3 Part 1.8 seems justified (meaning a single supplementary web plate with a maximum thickness equal to that of the column web). Additionally, the shear area A_{vc}^{*} of the column section in shear considered by Krawinkler's approach in Eq. (12) is more appropriate for use than the shear area A_{vc} of Eurocode 3 (which here seems too large). Moreover, in the absence of transversal stiffeners on the prolongation of the beam flanges, one should not forget that the angular distortion of the panel includes the usual one distortion due to the shearing of the panel and that one due to the local traction and compression effects on the column web (according to Eq. (14)). In fact, this study has proven that these effects on the total value of the angular stiffness are far from negligible.

(2) With regard to the resistance of the panel in shear, the authors recommend the use of the shear area A_{vc}^{*} given by Eq. (12) of Krawinkler's model augmented by the entire area of the supplementary plates, regardless of whether they are on a single side or on two sides of the column web. Two relations for computing the resistance were set forth, in function of the dissipative concept used in the anti-seismic design of joints:

a. When the joint is not conceived as dissipative and, consequently, there is no question of accepting significant plastic distortions within the CWP, the elastic moment $M_{cw,y}$ (from Eq. (7) of Krawinkler's model) seems to be the most appropriate for the computation of the panel resistance, with A_{vc}^{*} increased by the total area of the supplementary plates.
b. In contrast, when the joint is designed as dissipative, Eq. (8) of Krawinkler's model (including $M_{cw,u}$ computed as before) permits the use of a more favourable value of the resistant moment $M_{cw,u}$, under the condition of accepting a certain plastic angular distortion consistent with the limitation imposed in Eurocode 8-1 for the column panel.

To conclude, a clarifying remark imposes itself for the realisation of the specimens: they were deliberately chosen on steel grades of S355 for the beams and S235 for the columns respectively, in order to concentrate the plastic deformations in the CWP and thus to study their behaviour up to the ultimate state. Accordingly, and for the most reinforced case, CP-IIPD, the moment resistance of the CWP is an important fraction of the total plastic moment of the adjacent beams ($2M_{pl,b}$) (for which the measured elastic limit for the steel was 380 N/mm²). In this manner, the ratio of the resistant moment of the CWP to that of the beams of the CP-IIPD specimen has the value: $\frac{M_{cw,y}}{2M_{pl,b}} = \frac{521,8}{2 \times 380} = 0.69$. This ratio has a value of 0.29 for the reference specimen CP-R.

When considering practical seismic design, with connections conceived as dissipative, it is convenient that the ratio $M_{cw,u} / (2M_{pl,b})$ is not less than 0.8 as this was recommended by some norms (for example the AISC).

If the practical context of seismic design is considered, with connections conceived as dissipative, it is convenient that the ratio $M_{cw,u} / (2M_{pl,b})$ not be less than 0.8, as this was recommended by some norms (for example the AISC). Thus, it becomes clear that to satisfy such a criterion in certain design situations, the design engineer could be led to using appropriate steel grades (for example S355 or S460 for columns and S235 for the beams – contrary to the situation of this study) and probably to using supplementary plates, as computed from the equations mentioned in this article, particularly Eq. (8).

Acknowledgements

The research reported herein was supported by the World Bank and Romanian Government by the Ministry of Research and Education within the research contract « Reliability of Building Structures in High Risk Seismic Regions » CNCSIS / grant no. 16.

References

AISC (2004), Seismic Provisions for Structural Steel Buildings (Draft) – Public review III, (American Institute of Steel Construction), Inc. Chicago, Illinois, USA, November.

CEN (European Committee for Standardisation) (2003), Eurocode 3,-Part 1-1. 2003 EUROCODE 3: Design of Steel Structures – General rules and rules for buildings. Final Draft (stage 49), Brussels, November.

CEN (European Committee for Standardisation) (2003), Eurocode 8-Part 1. Design of structures for earthquake resistance – General rules, seismic actions and rules for buildings. Draft n°6 (stage 49), Brussels, January.

CEN (European Committee for Standardisation) (2003), Eurocode 3,-Part 1-8. 2003 EUROCODE 3: Design of Steel Structures. Design of Joints. Draft: May 2003 (stage 49),; Brussels, May.

Dubina, D., Ciutina, A. and Stratan, A. (2002), "Cyclic tests on bolted steel and composite double-sided beam-to-column joints", *Steel & Composite Structures*, **2**(2), 147-160.

Dubina, D., Ciutina, A. and Stratan, A. (2001), "Cyclic tests on double-sided beam-to-column joints", *J. Struct. Eng.*, **127**(2), 129-137.

El-Tawil, S., Mikesell, T., Vidarsson, E. and Hunnath, S. (1998), "Strength and ductility of FR welded-bolted connections", SAC Joint Venture, report n°BD-98/01.

European Commission for Constructional Steelwork ECCS; (1986), Recommended Testing Procedures for Assessing the Behaviour of Structural Elements under Cyclic Loads, European Convention for Constructional Steelwork, Technical Committee 1, TWG 1.3 – Seismic Design, No.45.

Krawinkler, H., Bertero, V. and Popov, E. (1971), "Inelastic behavior of steel beam-to-column subassemblages", Report No. EERC 71/07, University of California, Berkley, CA.

Krawinkler, H. (1978), "Shear in beam-column joints in seismic design of steel frames", *Eng. J.*, AISC, **3**, 82-91.

Lu, L.-W., Ricles, J., Changshi, M. and Fisher, J., (2000), "Critical issues in achieving ductile behaviour of welded moment connections", *J. Construct. Steel Res.*, **55**(1-3), 325-341.

Schneider, S. and Amidi, A. (1998), "Seismic behavior of steel frames with deformable panel zones", *J. Struct. Eng.*, **124**(1), 35-43.

Simões, R., Simões da Silva, L. and Cruz, P. (1999), "Experimental models of end-plate beam-to-column composite connections", *Proc. 2nd European Conf. on Steel Structures*, EUROSTEEL.99, Praha, Czech Republic, 625-629.

Notation

a : horizontal dimension of the panel zone
A_{vc} : shear area of the column
A[%] : elongation at rupture of steel samples
b : vertical dimension of the panel zone
E : Young's Modulus for steel
f_y : yielding resistance of steel
G : shear modulus of steel
f_u : ultimate resistance of steel
M_b : end bending moment a connected beam
M_{CWP} : web panel moment resistance
$M_{CWP\,y}$: conventional yielding web panel moment resistance
M_{sh} : strain-hardening moment

P : column axial load
V_c : column shear force
V_{wp} : CWP shear force
z : level arm of the CWP
β : transformation parameter
Δ_i : relative displacement recorded by the transducer i
γ : CWP distortion
γ_y : conventional yielding CWP distortion

CC